

Testing LHT at the LHC Run-II

Qing-Hong Cao,^{1,2,3,*} Chuan-Ren Chen,^{4,†} and Yandong Liu^{1,‡}

¹*Department of Physics and State Key Laboratory of Nuclear Physics and Technology, Peking University, Beijing 100871, China*

²*Collaborative Innovation Center of Quantum Matter, Beijing 100871, China*

³*Center for High Energy Physics, Peking University, Beijing 100871, China*

⁴*Department of Physics, National Taiwan Normal University, Taipei 116, Taiwan*

We study the Littlest Higgs model with T-parity (LHT) in the process of $pp \rightarrow W_H^+ W_H^- \rightarrow W^+ W^- A_H A_H$ at the 14 TeV LHC. With the W -jet tagging technique, we demonstrate that the bulk of the model parameter space can be probed at the level of more than 5σ in the signature of two fat W -jets plus large missing energy. Furthermore, we propose a novel strategy of measuring the principle parameter f that is crucial to testify the LHT model and to fix mass spectrum, including dark matter particle. Our proposal can be easily incorporated into current experimental program of diboson searches at the LHC Run-II.

Motivation: The mystery of why the mass of Higgs boson is at the weak scale remains after the Higgs discovery at the Large Hadron Collider (LHC). One possibility is given in the framework of Little Higgs models in which the Higgs boson emerges as a pseudo Nambu-Goldstone boson in the mechanism of collective symmetry breaking [1, 2]. The original construction of Little Higgs model suffers severely from electroweak precision tests that demand the collective symmetry breaking scale $f (= \Lambda/4\pi)$ to be large [3]. Therefore, the model reintroduces the fine-tuning and has little relevance to the current high energy collider physics program. The stringent constants can be naturally released when a discrete symmetry, called T-parity, is imposed [4–6]. All the corrections to electroweak observables are loop-induced. The value of f , then, can be as low as 500 GeV [7], and the masses of new heavy resonances are below TeV.

In this Letter we consider the ‘‘Littlest’’ Higgs model with T-parity (LHT), which is based on an $SU(5)/SO(5)$ nonlinear sigma model whose low energy Lagrangian is described in details in Ref. [8–10]. In the model under the T-parity transformation the SM particles are neutral while all the new particles are odd, except a top quark partner that cancels out the SM top quark’s contribution to the quadratic divergence in radiative corrections of mass parameter of the Higgs boson. The characteristics of the LHT are the dependence of few free parameters and the tight mass relation between heavy gauge bosons. For example, after the electroweak symmetry breaking, the masses of the T-parity partners of the photon (A_H) and W -boson (W_H) are generated as

$$M_{A_H} = \frac{g'f}{\sqrt{5}} \left(1 - \frac{5v^2}{8f^2}\right), \quad M_{W_H} = gf \left(1 - \frac{v^2}{8f^2}\right), \quad (1)$$

where v is the vacuum expectation value, and g and g' are the gauge couplings of $SU(2)_L$ and $U(1)_Y$, respectively. Because of the smallness of the $U(1)_Y$ gauge coupling constant g' , the T-parity partner of the photon A_H tends to be the lightest T-odd particle (LTP) in the LHT, which serves the dark matter (DM) candidate [11]. Given

the $SU(2)_L$ gauge coupling constant g and the vacuum expectation value v ($\simeq 246$ GeV) being measured in SM electroweak processes, the measurement of M_{W_H} could determine the value of f , the most important parameter of the LHT model. That in turn determines M_{A_H} (the DM mass), which is crucial for other experiments of dark matter searches, e.g. direct and indirect searches for dark matter. We demonstrate that the scale f can be determined through the production of charged heavy gauge boson pair ($W_H^+ W_H^-$) at the LHC.

The W_H boson almost entirely decays into a pair of W and A_H bosons in the LHT model [12]. Therefore, the collider signature of the $W_H^+ W_H^-$ production is controlled by decay products of the W bosons from the W_H decays. Both the leptonic and hadronic decay of the W bosons in the $W_H^+ W_H^-$ production have been studied in Refs. [12, 13], which pointed out that, owing to invisible DM particles in the final state, the event reconstruction is difficult. For example, one immediately confronts two difficulties that preclude the event reconstruction in the hadronic mode: i) unknown DM mass and undetectable DM momentum; ii) the W -boson being highly boosted such that its decay product tend to be highly collimated and hard to be isolated. We propose a novel method to overcome those difficulties to measure M_{W_H} , M_{A_H} and f in the process of $pp \rightarrow W_H^+ W_H^- \rightarrow W^+ (\rightarrow jj) W^- (\rightarrow jj) A_H A_H$; see Fig. 1.

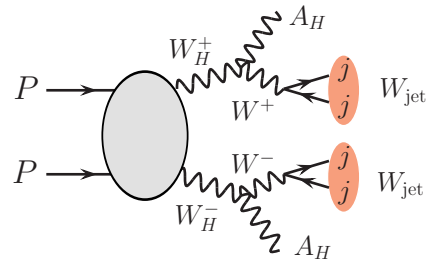


FIG. 1. Pictorial illustration of the pair production and decay of W_H at the LHC.

The Method: We begin with the difficulty in the W -boson reconstruction. In the allowed parameter space of f the W_H boson is much heavier than the W and A_H bosons. Thus, the W boson from the W_H decay is highly boosted such that the two jets of the W boson decay tend to be collimated and form one fat jet in the detector. We name it as a W -jet (W_J). The substructure of the W -jet provides a powerful tool to detect the signal event and suppress background significantly; for example, when the transverse momentum (p_T) of the W boson is larger than 200 GeV, the boosted jet algorithm, used to identify W jets, becomes more efficient than the reconstruction of a W boson from two isolated jets [14]. The W -jet technique has been successfully used in searching for new resonances in the diboson channel by the ATLAS [15] and CMS [16, 17] collaborations.

Next we deal with the unknown mass of the invisible

DM particle. The general challenge of determining the mass of new heavy particles that decay into DM is that no mass resonance can be reconstructed because of the lack of kinematic information of DM candidates. In the SM processes with two or less neutrinos in the final state, one might be able to use on-shell conditions of those intermediate particles to reconstruct the momenta of the missing neutrinos [18, 19]; for example, the momentum of the neutrino in the top-quark decay, $t \rightarrow bW^+(\rightarrow \ell^+\nu)$, can be solved from the on-shell condition of the W boson [20]. Unfortunately, the on-shell technique does not apply here because M_{A_H} is unknown. With two DM particles and no neutrino in the final state, the so-called M_{T2} variable is designed in such a way that its distribution will be bound from above by the true mass of the mother particle [21]. The definition is given as

$$m_{T2}(p_{\text{vis}}^{(1)}, p_{\text{vis}}^{(2)}, \vec{\mathcal{E}}_T; m_{\text{inv}}) \equiv \min_{\vec{\mathcal{E}}_T = \vec{\mathcal{E}}_T^{(1)} + \vec{\mathcal{E}}_T^{(2)}} \left[\max \left\{ m_T(p_{\text{vis}}^{(1)}, \vec{\mathcal{E}}_T^{(1)}; m_{\text{inv}}), m_T(p_{\text{vis}}^{(2)}, \vec{\mathcal{E}}_T^{(2)}; m_{\text{inv}}) \right\} \right], \quad (2)$$

where

$$m_T(p_{\text{vis}}^i, \vec{\mathcal{E}}_T^i; m_{\text{inv}}) \equiv \sqrt{m_{\text{inv}}^2 + m_{\text{vis}}^2 + 2(E_T^{\text{vis}} \mathcal{E}_T^{(i)} - \vec{p}_{\text{vis}}^i \cdot \vec{\mathcal{E}}_T^i)}, \quad (3)$$

is the transverse mass of the visible cluster p_{vis}^i and the missing transverse momentum $\vec{\mathcal{E}}_T^i$. Here, m_{vis} denotes the invariant mass of visible cluster and m_{inv} is the mass of missing particle. In our case, the visible cluster in Eq. (2) refers to the W -jet and the endpoint of M_{T2} distributions in the upper end determines M_{W_H} when the true mass of the missing dark matter M_{A_H} is inputted. The M_{T2} method is theoretically ideal, however, because there is a lack of mass information of dark matter particle, its application of determining the mass of mother particle is still limited.

Thanks to the strong correlation between masses of heavy gauge bosons in the LHT model,

$$M_{W_H} = (\sqrt{5}g/g')M_{A_H} \approx 4.2M_{A_H}, \quad (4)$$

we introduce a new variable M_{T2}^0 to determine the value of f in the $W_H^+W_H^-$ production without knowing M_{A_H} . The variable is defined as

$$M_{T2}^0 \equiv m_{T2}(p_{\text{vis}}^{(1)}, p_{\text{vis}}^{(2)}, \vec{\mathcal{E}}_T; m_{\text{inv}} = 0), \quad (5)$$

which, in the limit of $M_{W_H} \gg M_{A_H, W}$, exhibits a distribution with an upper edge at [22]

$$M_{T2}^{\text{End0}} \simeq M_{W_H} - \frac{M_{A_H}^2}{M_{W_H}} \left[1 + \frac{M_W^2}{M_{W_H}^2} + \mathcal{O}\left(\frac{M_{W, A_H}^4}{M_{W_H}^4}\right) \right]$$

$$\begin{aligned} &\approx M_{W_H} - \frac{M_{A_H}^2}{M_{W_H}} = \frac{5g^2 - g'^2}{5g} f \left(1 - \frac{9v^2}{8f^2} \right) \\ &\approx \frac{5g^2 - g'^2}{5g} f \sim 0.62f. \end{aligned} \quad (6)$$

The measurement of M_{T2}^{End0} determines the value of f , from which the masses of W_H and A_H bosons can be derived. One then can substitute the derived M_{A_H} into the M_{T2} variable given in Eq. (2) to plot the M_{T2} distribution with the upper ending point being the mass of W_H . In this way a consistency check of the mass relation given in Eq. (4) can be made, which is of great importance to verify the LHT model. Moreover, one can examine the leptonic mode, $W_H W_H \rightarrow W^+(\rightarrow \ell^+\nu)W^-(\rightarrow \ell'^-\bar{\nu})A_H A_H \rightarrow \ell^+\ell'^- + \mathcal{E}_T$, to cross-check the LHT model.

Collider Simulation: The collider signature of interests to us is two W -jets with large missing momentum $\cancel{\mathcal{E}}_T$ arising from the two invisible A_H 's. The $\cancel{\mathcal{E}}_T$ plays the key role of triggering the signal events. In order to mimic the signal events, the SM background should consist of W or Z bosons. We consider SM backgrounds as follows: i) the pair production of WW , WZ and ZZ bosons; ii) $t\bar{t}$ productions; iii) the associated production of a W boson and multiple jets (denoted by W +jets); iv) the associated production of a Z boson and multiple jets (Z +jets). The W +jets, Z +jets and triple gauge boson productions are negligible after kinematics cuts. We generate the $W_H^+W_H^-$ production and background events at the parton level using MadEvent [23] at the 14 TeV LHC and pass events to Pythia [24] for showering and hadronization. We

TABLE I. The numbers of the signal and background events after a series of kinematic cuts at the 14 TeV LHC with an integrated luminosity of 100 fb^{-1} . For the signal event $\kappa = 3$.

	$f = 0.5 \text{ TeV}$	$f = 1.0 \text{ TeV}$	$f = 1.5 \text{ TeV}$	$t\bar{t}$	WW	WZ	ZZ
No cut	88698	2735.04	244.32	5.5×10^7	9.54×10^6	4.36×10^6	1.25×10^6
\cancel{E}_T , W_{jet} -tagging and M_{JJ}	295.33	38.51	5.51	13.31	4.77	6.43	1.17

utilize Delphes [25] to simulate detector smearing effects in accord to a fairly standard Gaussian-type detector resolution given by $\delta E/E = \mathcal{A}/\sqrt{E/\text{GeV}} \oplus \mathcal{B}$, where \mathcal{A} is a sampling term and \mathcal{B} is a constant term. For leptons we take $\mathcal{A} = 5\%$ and $\mathcal{B} = 0.55\%$, and for jets we take $\mathcal{A} = 100\%$ and $\mathcal{B} = 5\%$. We also impose the lepton veto if the lepton has transverse momentum p_T^ℓ greater than 20 GeV, rapidity $|\eta_\ell| \leq 2.5$ and its overlap with jets $\Delta R_{j\ell} = \sqrt{(\Delta\eta)^2 + (\Delta\phi)^2} \geq 0.4$. The missing transverse momentum (\cancel{E}_T) is then defined to balance the total transverse momentum of visible objects.

A 2-pronged boosted W -jet is tagged using the so-called ‘‘mass-drop’’ technique with asymmetry cut introduced in Ref. [26]. The W -jet reconstruction is performed using Cambridge/Aachen algorithm with Fastjet [27]. The distance parameter of 1.2 is adopted to cluster a fat jet that is initiated by the boosted W boson. We further require the invariant masses of those reconstructed fat 2-prong jets (M_J) within the following mass window [15]:

$$m_W - 13 \text{ GeV} \leq M_J \leq m_W + 13 \text{ GeV}, \quad (7)$$

where $m_W = 80.425 \text{ GeV}$ is the mass of W -boson. After p_T ordering, we plot the p_T distributions of the leading W -jet and the subleading W -jet of the signal and background events in Fig. 2(a) and 2(b), respectively. Since the W -jets in the signal events arise from the heavy W_H decays, their p_T distributions are in general harder than those of the SM background events. We demand the leading W -jet (J_1) and the subleading W -jet (J_2) to satisfy

$$p_T^{J_1} \geq 200 \text{ GeV}, \quad p_T^{J_2} \geq 100 \text{ GeV}, \quad |\eta^{J_{1,2}}| \leq 3, \quad (8)$$

to suppress the SM background. The numbers of events of the signal and background after the above cut are shown in the third row of Table I with an integrated luminosity of 100 fb^{-1} . For illustration we choose three benchmark values of f (0.5 TeV, 1 TeV, 1.5 TeV). For simplification we fix $\kappa = 3$ assuming the masses of T-odd fermions, $M_{f_\pm} \simeq \sqrt{2}\kappa f$, are much heavier than W_H . We emphasize that the cut efficiencies obtained above depend mainly on the mass split between W_H and A_H .

We take the advantage of the large missing transverse momentum of the signal events to trigger the signal events and reject the SM backgrounds; see Figure 2(c). We impose a hard cut on the missing transverse momentum as $\cancel{E}_T \geq 400 \text{ GeV}$. Furthermore, the two W -jets in the signal events originate from two W_H 's and exhibit a

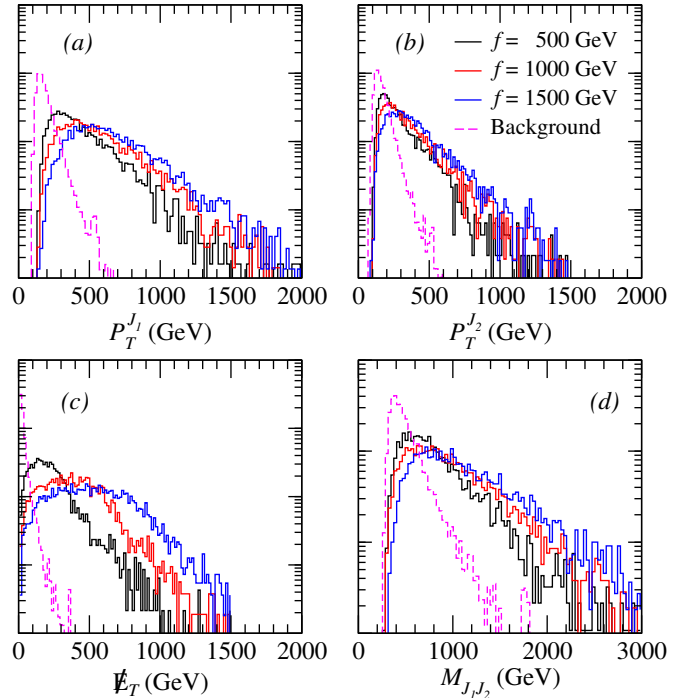


FIG. 2. Normalized distribution of the signal events ($f = 0.5, 1.0, 1.5 \text{ TeV}$) and background events: p_T of the leading W -jet (a) and the subleading W -jet (b); the invariant mass of the two W -jets (c); the missing transverse momentum (d).

large invariant mass (M_{JJ}) as shown in Figure 2(c). We thus impose a hard cut on $M_{J_1 J_2}$ as following:

$$M_{J_1 J_2} \geq 500 \text{ GeV}, \quad (9)$$

which efficiently reduces the SM backgrounds; see the third row in Table I.

Given the cut efficiencies of both the signal and backgrounds, we are in a position to estimate the potential of the LHC in the search for $W_H^+ W_H^-$ pair production with the signature of two fat W -jets and large missing energy. We calculate the 5σ discovery potential using

$$\sqrt{-2 \left[(n_b + n_s) \ln \left(\frac{n_b}{n_s + n_b} \right) + n_s \right]} = 5 \quad (10)$$

where n_s denotes the number of the signal events while n_b the number of the background events [28].

The 5σ sensitivity in the plane of f and κ is shown in Fig. 3 for three benchmark integrated luminosities of $\mathcal{L} = 100 \text{ fb}^{-1}$, 300 fb^{-1} and 3000 fb^{-1} . For $\kappa \gtrsim 2.5$

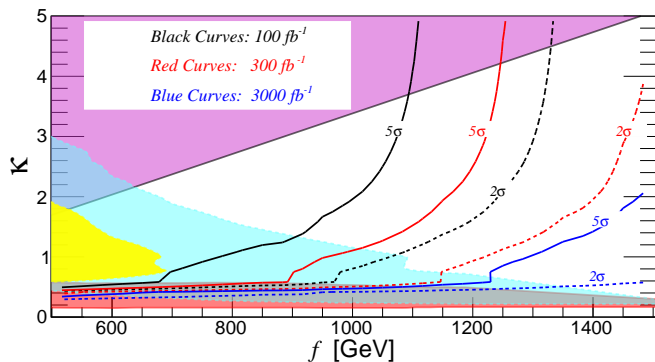


FIG. 3. The 5σ discovery potential (solid curves) and 2σ exclusion limit (dashed curves) of the $W_H^+ W_H^-$ pair production at the 14 TeV LHC with three integrated luminosities: $\mathcal{L} = 100 \text{ fb}^{-1}$ (black), 300 fb^{-1} (red) and 3000 fb^{-1} (blue). The shaded regions are excluded by the low energy experiments and the LHC Run-1 data [10]; see text for more details.

the discovery potential is not sensitive to f . It is owing to the fact that the T -odd fermion’s contribution to the $W_H W_H$ pair production is highly suppressed for a large value of κ . As a result the production cross section depends mainly on the f rather than κ . Obviously a large amount of parameter spaces could be probed at the high luminosity (HL, 3000 fb^{-1}) LHC. For comparison, we also plot the current experimental limits [10]: the magenta region denotes the indirect constraint from the four-fermion contact operators $eedd$; the blue region is constrained by the Jet and \cancel{E}_T data, the yellow region is bounded by the Leptons, Jets and \cancel{E}_T and the red region at the bottom is excluded by the Monojet and \cancel{E}_T ; see Ref. [10] for details. Most of the allowed parameter spaces can be probed in the $W_H W_H$ pair production at the high luminosity LHC with an integrated luminosity of 3000 fb^{-1} , see the blue solid line.

The $W_H^+ W_H^-$ pair production is also a good process for excluding the parameter space of the LHT model. Figure 3 also shows the 2σ exclusion limits in the plane of f and κ , which are calculated using

$$\sqrt{-2 \left(n_b \ln \frac{n_s + n_b}{n_b} - n_s \right)} = 1.96. \quad (11)$$

The red (black, blue) dashed curve denotes the exclusion limit at the LHC with an integrated luminosity of 100 fb^{-1} (300 fb^{-1} , 3000 fb^{-1}). If, unfortunately, no excess were observed in the $W_H^+ W_H^-$ pair production at the HL-LHC, then we conclude that almost entirely allowed parameter space of $f \leq 1.5 \text{ TeV}$ by the current data would be ruled out; see the blue dashed curve. A large f , say $f > 1.5 \text{ TeV}$, would reintroduce Little Hierarchy problem which weaken the original motivation of the LHT model.

The measurements of f and M_{W_H} : Next we demonstrate that the parameters f , M_{W_H} and M_{A_H} in the

LHT model can be determined from the $M_{T_2}^0$ distribution where $M_{T_2}^0 = m_{T_2}(p_{J_1}, p_{J_2}, \cancel{E}_T; M_{A_H} = 0)$, where p_{J_1} and p_{J_2} are the momentum of two W -jets. Figure 4(a) displays the $M_{T_2}^0$ distribution for $f = 500 \text{ GeV}$ and 1000 GeV , respectively. Only statistical uncertainty is included in the plot.

The value of $M_{T_2}^{\text{End}0}$, the endpoint of $M_{T_2}^0$, is extracted out by a “kink-to-bump” method [29]. The method utilizes two straight lines to fit the $M_{T_2}^0$ distribution around the edge to find the kink position. A global fitting then gives rise to a likelihood function peaking around the true kink position. We obtain the values of $M_{T_2}^{\text{End}0}$ as 325 (653) GeV for $f = 500$ (1000) GeV, respectively. The theoretical values predicted by the LHT model in Eq. (6) are 302 GeV and 611 GeV, respectively. The measured values are in good agreement with the LHT predictions. Figure 4(b) plots the value of $M_{T_2}^{\text{End}0}$ as a function of f . The solid curve represents the $M_{T_2}^{\text{End}0}$ obtained from fitting while the dashed curve denotes the theoretical relation. The $\sim 10\%$ discrepancy can be treated as the uncertainty of our method. In practice one could use M_{A_H} derived from $M_{T_2}^{\text{End}0}$ to reconstruct the M_{T_2} distribution and then measure M_{W_H} from its endpoint.

The M_{W_H} and M_{A_H} can be calculated directly from f once the value of f is determined from $M_{T_2}^{\text{End}0}$ measurement. So far only the statistical uncertainty is considered

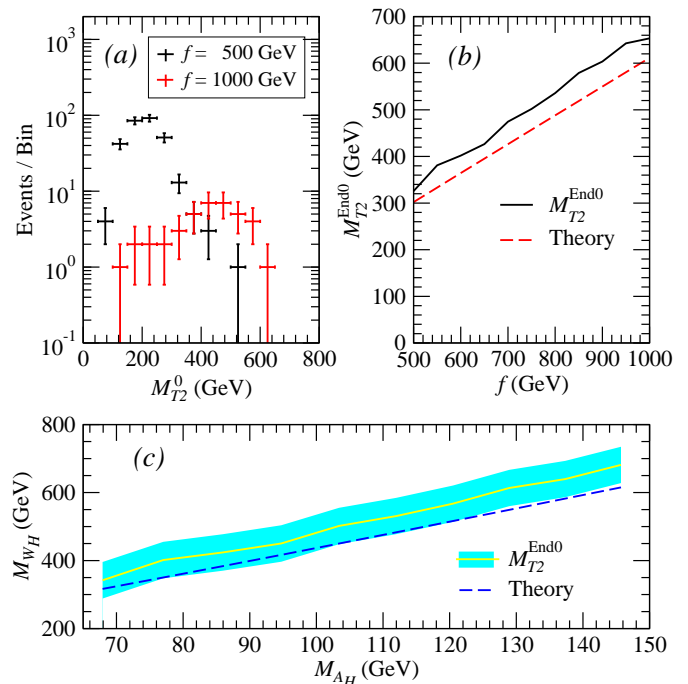


FIG. 4. (a) The $M_{T_2}^0$ distribution for $f = 0.5$ (1.0) TeV for an integrated luminosity of 100 fb^{-1} ; (b) the $M_{T_2}^{\text{End}0}$ determined in the so-called “kink-to-bump” method [29] versus the scale f (solid curve) while the true theoretical value of $M_{T_2}^{\text{End}0}$ is also plotted for comparison (dashed curve).

in the calculation. The systematical uncertainties are expected to be much larger than the statistical uncertainties, however. The light blue band in the Figure 4(c) shows the calculated W_H and A_H when a ± 50 GeV uncertainty is taken into account in M_{T2}^{End0} measurement, which is in good agreement with the unique mass relation between T-odd heavy gauge bosons in LHT model shown by the dashed line.

Summary and Discussion: Little Higgs Model with T-parity provides an explanation for the Higgs mass being at the weak scale and a suitable candidate for dark matter particle. With the aid of jet substructure, LHC has the capability of probing most of the parameter space with W_H pair production, using the hadronic final state. We propose a strategy to determine the most important parameter, the energy scale f , using the M_{T2} analysis. The unique mass relation between the heavy gauge bosons W_H and A_H can be tested as well.

A pair of boosted W -jets is an important channel to search for new resonance at the LHC Run-II [15–17]. However, when dark matter is involved in the decay products, resonances of diboson pairs will not be reconstructed and our approach can be easily incorporated. As the 2 TeV diboson anomaly found in Run-I data is not confirmed by the Run-II data [30], we recommend that the data should be revisited with missing energy analysis, as we have shown in this letter.

Acknowledgments: CRC would like to acknowledge the support of National Center for Theoretical Sciences (NCTS). The work of QHC and YDL is supported in part by the National Science Foundation of China under Grand No. 11275009. The work of CRC is supported in part by the National Science Council of R.O.C. under Grants No. NSC 102-2112-M-003-001-MY3.

* qinghongcao@pku.edu.cn

† crchen@ntnu.edu.tw

‡ ydliu@pku.edu.cn

- [1] N. Arkani-Hamed, A. G. Cohen, and H. Georgi, Phys. Lett. **B513**, 232 (2001), hep-ph/0105239.
- [2] N. Arkani-Hamed, A. G. Cohen, E. Katz, and A. E. Nelson, JHEP **07**, 034 (2002), hep-ph/0206021.
- [3] C. Csaki, J. Hubisz, G. D. Kribs, P. Meade, and J. Terning, Phys. Rev. **D67**, 115002 (2003), hep-ph/0211124.
- [4] H.-C. Cheng and I. Low, JHEP **09**, 051 (2003), hep-ph/0308199.
- [5] H.-C. Cheng and I. Low, JHEP **08**, 061 (2004), hep-ph/0405243.
- [6] I. Low, JHEP **10**, 067 (2004), hep-ph/0409025.
- [7] J. Hubisz, P. Meade, A. Noble, and M. Perelstein, JHEP **01**, 135 (2006), hep-ph/0506042.
- [8] J. Hubisz and P. Meade, Phys. Rev. **D71**, 035016 (2005), hep-ph/0411264.
- [9] A. Belyaev, C.-R. Chen, K. Tobe, and C. P. Yuan, Phys. Rev. **D74**, 115020 (2006), hep-ph/0609179.
- [10] J. Reuter, M. Tonini, and M. de Vries, JHEP **02**, 053 (2014), 1310.2918.
- [11] M. Asano, S. Matsumoto, N. Okada, and Y. Okada, Phys. Rev. **D75**, 063506 (2007), hep-ph/0602157.
- [12] Q.-H. Cao and C.-R. Chen, Phys. Rev. **D76**, 075007 (2007), 0707.0877.
- [13] D. Song-Ming, G. Lei, L. Wen, M. Wen-Gan, and Z. Ren-You, Phys. Rev. **D86**, 054027 (2012), 1208.5532.
- [14] V. Khachatryan et al. (CMS), JHEP **12**, 017 (2014), 1410.4227.
- [15] G. Aad et al. (ATLAS) (2015), 1506.00962.
- [16] V. Khachatryan et al. (CMS), JHEP **08**, 173 (2014), 1405.1994.
- [17] C. Collaboration (CMS) (2015), CMS-PAS-EXO-15-002.
- [18] E. L. Berger, Q.-H. Cao, C.-R. Chen, G. Shaughnessy, and H. Zhang, Phys. Rev. Lett. **105**, 181802 (2010), 1005.2622.
- [19] H. Zhang, E. L. Berger, Q.-H. Cao, C.-R. Chen, and G. Shaughnessy, Phys. Lett. **B696**, 68 (2011), 1009.5379.
- [20] Q.-H. Cao, R. Schwienhorst, J. A. Benitez, R. Brock, and C. P. Yuan, Phys. Rev. **D72**, 094027 (2005), hep-ph/0504230.
- [21] C. G. Lester and D. J. Summers, Phys. Lett. **B463**, 99 (1999), hep-ph/9906349.
- [22] W. S. Cho, K. Choi, Y. G. Kim, and C. B. Park, JHEP **02**, 035 (2008), 0711.4526.
- [23] J. Alwall, P. Demin, S. de Visscher, R. Frederix, M. Herquet, F. Maltoni, T. Plehn, D. L. Rainwater, and T. Stelzer, JHEP **09**, 028 (2007), 0706.2334.
- [24] T. Sjöstrand, S. Ask, J. R. Christiansen, R. Corke, N. Desai, P. Ilten, S. Mrenna, S. Prestel, C. O. Rasmussen, and P. Z. Skands, Comput. Phys. Commun. **191**, 159 (2015), 1410.3012.
- [25] J. de Favereau, C. Delaere, P. Demin, A. Giammanco, V. Lematre, A. Mertens, and M. Selvaggi (DELPHES 3), JHEP **02**, 057 (2014), 1307.6346.
- [26] J. M. Butterworth, A. R. Davison, M. Rubin, and G. P. Salam, Phys. Rev. Lett. **100**, 242001 (2008), 0802.2470.
- [27] M. Cacciari, G. P. Salam, and G. Soyez, Eur. Phys. J. **C72**, 1896 (2012), 1111.6097.
- [28] G. Cowan, K. Cranmer, E. Gross, and O. Vitells, Eur. Phys. J. **C71**, 1554 (2011), [Erratum: Eur. Phys. J. **C73**, 2501 (2013)], 1007.1727.
- [29] D. Curtin, Phys. Rev. **D85**, 075004 (2012), 1112.1095.
- [30] The ATLAS collaboration (2015), ATLAS-CONF-2015-073.